External Stress Effect on Microstructure and Transformation Plasticity of Hot Work Tool Steel during Quenching

R. K. Janutienė[a,1] and R. K. Dičkuvienė[b,2]

[a] Kaunas University of Technology, Kaunas, Lithuania

[b] Lithuanian Energy Institute, Kaunas, Lithuania

[1] raskand@ktu.lt

[2] regina@isag.lei.lt

Влияние напряжений от внешних нагрузок на микроструктуру и пластичность при фазовом превращении жаропрочной инструментальной стали при закалке

Р. К. Жанутиене[a], Р. К. Дицкувиене[б]

[a] Каунасский технологический университет, Каунас, Литва

[б] Литовский энергетический институт, Каунас, Литва

Исследуется изменение пластичности и микроструктуры жаропрочной инструментальной стали при мартенситном превращении. Образцы подвергались аустенитизации и закалке на воздухе. В процессе охлаждения их нагружали статическим изгибом с номинальным напряжением 100 МПа по трем схемам: статический изгиб образцов после их изъятия из печи, при этом отмечались деформация исходного аустенита и формирование мартенсита под нагрузкой; изгиб после начала мартенситного превращения с деформацией мартенсита; разгрузка с момента начала мартенситного превращения с преобладающей деформацией аустенита, при этом измерялась деформация при разгрузке. При охлаждении образцов до комнатной температуры измерялась величина их пластического прогиба. Показано, что мартенситное превращение характеризуется существенным повышением пластичности. Различное влияние на мартенситное превращение растягивающих и сжимающих напряжений оценивалось путем измерения деформации образцов при разгрузке. Микроструктура растянутых и сжатых поверхностей образцов исследовалась методами рентгеновской дифрактометрии, электронной микроскопии и электронно-дисперсионной спектроскопии.

Ключевые слова: мартенситное превращение, жаропрочная сталь, микроструктура, пластичность, термообработка.

Introduction. The accuracy in size of hot-work tools is a very important question in manufacturing of forgings [1, 2]. The hot-work tools can be affected by various stresses originating during the long-term exploitation of tool and the precise measurement of a part can be lost. Long-term exploitation is related with spontaneous tempering which occurs during contact between tool and hot material, causing diffusion of carbon and alloying elements [1]. The stresses occurring in the steel and therefore coming plastic deformations of parts are related with the following processes [3–5]:

(i) residual stresses remained after machining;

(ii) microstructural stresses caused by constituents volume mismatch in microstructure after austenite–martensite transformations;

(iii) stress relaxation under the heat effect, especially when transformation plasticity proceeds;

(iv) thermal stresses related with different ratios of thermal expansion of martensite, austenite, and other constituents.

The regimes of quenching and tempering used for tools, simple or complex geometry of parts also could be mentioned, e.g., tools with high length-to-diameter ratio have a tendency to quenching distortion. Such distorted parts could be easily straightened out by tension, bending or other methods performing during transformation plasticity effect. Therefore the research of properties of each steel grade during thermal operations is very important.

The variation in plasticity of different sorts of steel during martensitic transformation and following tempering can be multiform [6–8].

The transformation plasticity of steel can be qualitatively assessed by comparing the plastic deflection of equal-sized specimens tested at certain transformations. Computing of the elastic modulus E_{tp} of transformation plasticity can provide a quantitative analysis of this effect [9]. Steel has the highest plasticity when it undergoes martensitic transformation, i.e., plasticity of the quenched specimen is greater from several to dozen times comparing to the one obtained after tempering. The value of transformation plasticity of quenched steel is directly related with carbon content [10]. Also, the transformation plasticity of steel is under the influence of the temperature of quenching and tempering, the content of alloying elements, etc. [9, 10].

In some cases, steel products and hot-work tools as well, are heat treated under the transformation plasticity effect for ensuring their dimensional accuracy, e.g., by fixing the shape, but unfortunately the results are often not satisfactory. The most common errors are too high temperatures for the start of air quenching that cause slight thermal stress, especially when cooling is asymmetrical. Also, the load force used for correction of geometric shape can be applied too early or too late considering on the start of martensitic transformation. Loss of transformation plasticity or self-deformation occurs because of varying of the intensity of ongoing martensitic transformation. The specimens may bend themselves even as they are not externally loaded or affected by thermal stresses [6, 11]. In order to make efficient use of the effect of transformation plasticity of precise steel production technology it is necessary to know the kinetics of transformation plasticity of each steel grade and its heat treatment peculiarities.

This work presents the investigation of transformation plasticity during martensitic transformation of the Swedish company Uddeholm hot-work tool steel Hotvar alloyed with chromium, molybdenum, and vanadium, used in hot-deformation dies, mould fabrication, etc.

1. **Experimental**. The chemical composition of the investigated steel is listed in Table 1.

T a b l e 1

Chemical Composition of Uddeholm Hotvar Steel (%)

C	Si	Mn	Cr	Mo	V	Fe
0.55	1.00	0.80	2.60	2.30	0.90	Bal.

The steel rods were used for manufacturing of the specimens of rectangular cross section and measurement of $100 \times 8 \times 6 \, \text{mm}^3$. The specimens were austenized at 1050, 1070, and 1090°C temperatures in the environment of protective gas of $N_2 + CO + CO_2$ and then air quenched. For the investigation of transformation plasticity effect, the austenized specimen was placed in the special bending device [10] and air quenched at the same time.

At the set temperature the specimen was loaded by bending load generated bending stress of 100 MPa and not exceeded yield strength $R_{p0.2}$ of steel at the certain temperature (yield strength of Hotvar is $R_{p0.2}$ = 1110 MPa at T = 550℃ [12]), then the plastic deflection of specimen was measured with accuracy of 0.01 mm until room temperature of specimen was reached. The ranges of bending test temperatures were:

(i) from 550℃ to room temperature (RT). The temperature 550℃ is an approximate temperature at which the specimen is placed in testing device and bending starts. This temperature was indicated by chromel-alumel thermocouple. At the start of bending, the deformation affects the initial structure (austenite). Then, under the effect of stresses the martensite transformation starts;

(ii) from 160–180℃ to RT. According the data of manufacture of the steel, the martensite start temperature M_s is in the range of 210–220℃ [12], so, at the moment of the beginning of deformation, the martensite transformation is already started;

(iii) from 550℃ to 160–180℃ temperature followed by free-load cooling to RT. This regime was chosen mainly to observe the self-deformation of specimen, when the initial structure (austenite) was deformed.

The bending load was chosen for the purpose of producing different types of stresses in the specimen. During bending, one part of the specimen was stretched, while the other was compressed. Effect of tension and compression on transformations of steel was observed. According to available literary data, transformations in steel can be influenced differently by the variant stress state [13, 14].

The temperature of specimen during heat treatment was measured by welded chromel-alumel thermocouple of 0.3 mm diameter, and the data were plotted together with the deflection curves.

After quenching the specimens were tested for heat treatment quality. Universal hardness meter VERZUS 750CCD for Rockwell hardness measurement was used.

The microstructural analysis was carried out on ZEISS EVO MA10 scanning electron microscope (SEM) in back scattering mode and operated at 20 kV. Heat or thermo-mechanically treated specimens were machine ground, polished using 1 μm diamond suspension, and etched in 3% Nital solution.

he XRD analysis was performed using a D8 Advance diffractometer (Bruker AXS, Karlsruhe, Germany) operating at the tube voltage of 40 kV and tube current of 40 mA. The X-ray beam was filtered with Ni 0.02 mm filter to select the CuK$_\alpha$ CuK wavelength (λ = 1.5406 Å). Diffraction patterns were recorded in a Bragg–Brentano geometry using a fast counting detector Bruker LynxEye based on the silicon strip technology. The specimens of metal and electrochemically extracted carbides were scanned over the range 2θ = 25–90° and 2θ = 3–100°, respectively, at a scanning speed of 6 deg/min using a coupled two theta/theta scan type.

The crystal lattice parameters of martensite phase were calculated using PowderCell program and Le Bail structureless whole pattern fitting algorithm [15].

Carbide phases were identified using search match program Bruker EVA and PDF-4 database [16].

The XRD analysis allowed identify the type of phases, content of retained austenite, and the parameters of lattice of martensite at the compressed and stretched surfaces of specimen.

2. **Results and Discussion**.

2.1. *Microstructural Analysis of Quenched Steel*. The steel containing vanadium has a very fine microstructure: grains are several micrometers in size, i.e., about the size of ASTM9 [17].

The analysis of quenched cross-cuts' microstructure has shown that after heat treatment the structure was formed mainly of lath martensite and retained austenite (in a very low content, as it will be discussed later) mixed with dispersive carbides (Fig. 1). The
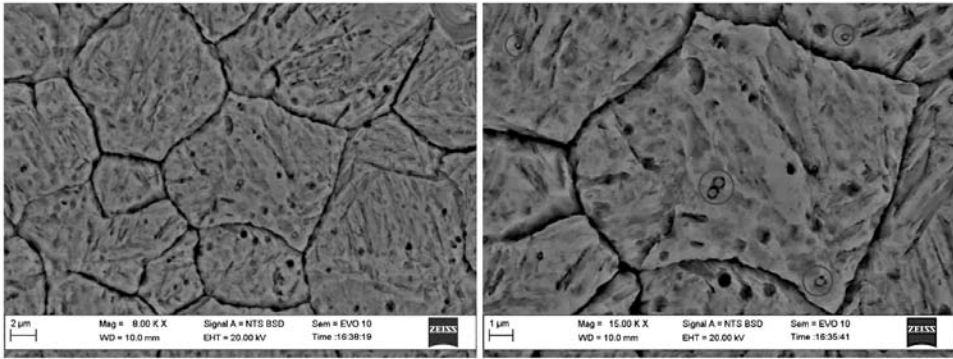
Fig. 1. SEM micrograph of air quenched Hotvar steel austenized at 1090°C.

martensite can be identified as grey brindle zones (some of them are marked with arrows) located in the austenite matrix with the primary grain boundaries.

The carbides are very small, less than 1 μm in diameter, highlighted with circles in Fig. 1. Elemental mapping by SEM with energy dispersive X-ray spectrometry (EDS) was used to reveal the carbides' type. It was found that the carbides mainly consisted of vanadium (Figs. 2 and. 3). Molybdenum could also be found in carbides, as SEM line scanning showed a slight increase of its amount in carbides, which was confirmed by the XRD analysis. The dominant presence of vanadium in carbides is clearly revealed by SEM elemental scanning of the area (Fig. 3).
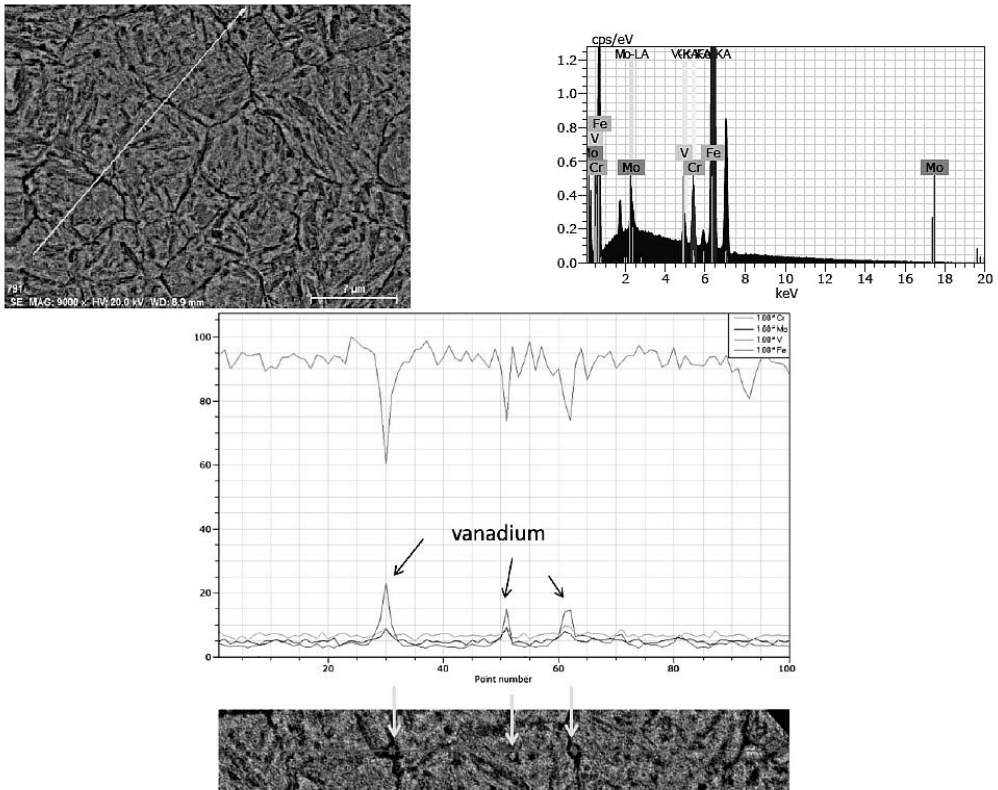

Fig. 2. Carbide SEM line scanning of air quenched Hotvar steel specimen austenized at 1050°C.

T a b l e 2

List of Carbides Detected in Hotvar Steel after Air Quenching from Different Temperatures

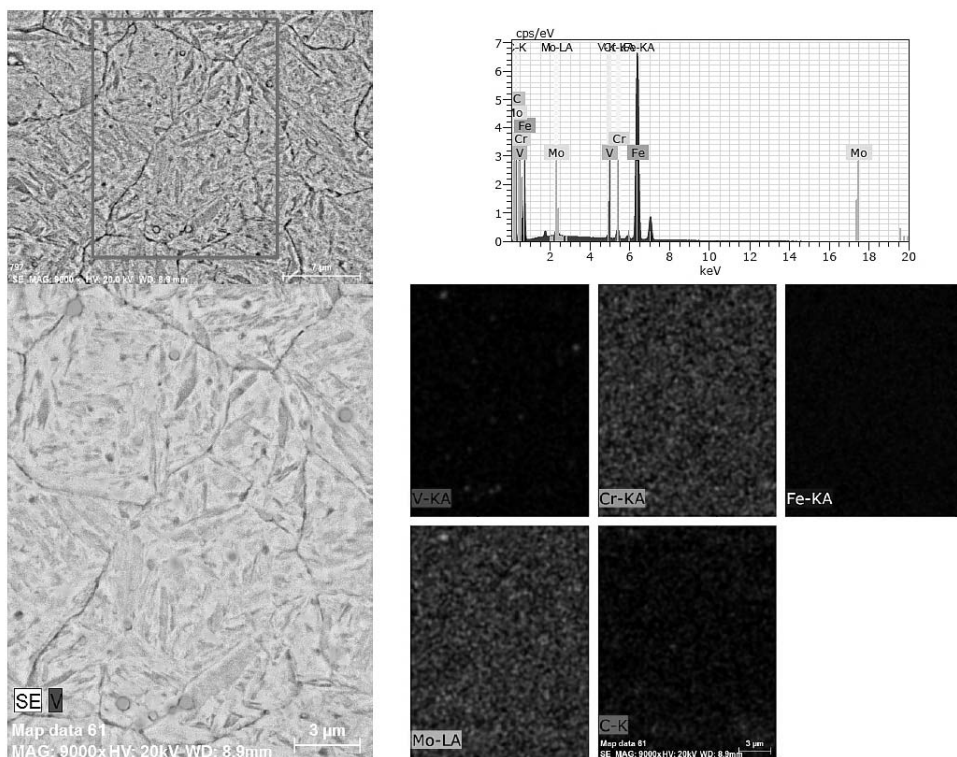| Air quenching temperature (℃)					
1050		1070		1090	
Matched materials					
Formula	$VC_{0.88}$	Formula	VC	Formula	$VC_{0.88}$
PDF number	77-2003	PDF number	73-476	PDF number	77-2003
Formula	VC	Formula	V_8C_7	Formula	V_8C_7
PDF number	73-476	PDF number	73-394	PDF number	73-394
Formula	V_8C_7	Formula	$VC_{0.88}$	Formula	VC
PDF number	73-394	PDF number	77-2003	PDF number	73-476
–	–	Formula	MoOC	Formula	MoOC
		PDF number	17-104	PDF number	17-104
–	–	Formula	Mo_2C	Formula	Mo_2C
		PDF number	15-457	PDF number	15-457

Fig. 3. Elemental mapping of air quenched Hotvar steel specimen austenized at 1050℃.

No significant differences between the microstructure of the cross-cuts from different quenching temperatures were observed.

The presence of vanadium in carbides was confirmed by the XRD analysis. The list of detected carbides depending on the austenizing temperature is presented in Table 2. The peaks were matched with the standard materials of PDF-4 database [16]. The list is given by the declining order of confidence.

However, detection of molybdenum in carbides was quite problematic, due to the lack of material for precise XRF quantitative analysis. XRD of carbides showed a possible peak of molybdenum carbide (Fig. 4). It looks like being stuck to clearly expressed peak of vanadium carbide. The peak of possible molybdenum carbide in XRD curves was marked by arrows (Fig. 4). Also, it was observed that the intensity of carbides peaks increased by lowering the heating temperature. This may attributed to the changes of solubility of elements in the matrix.
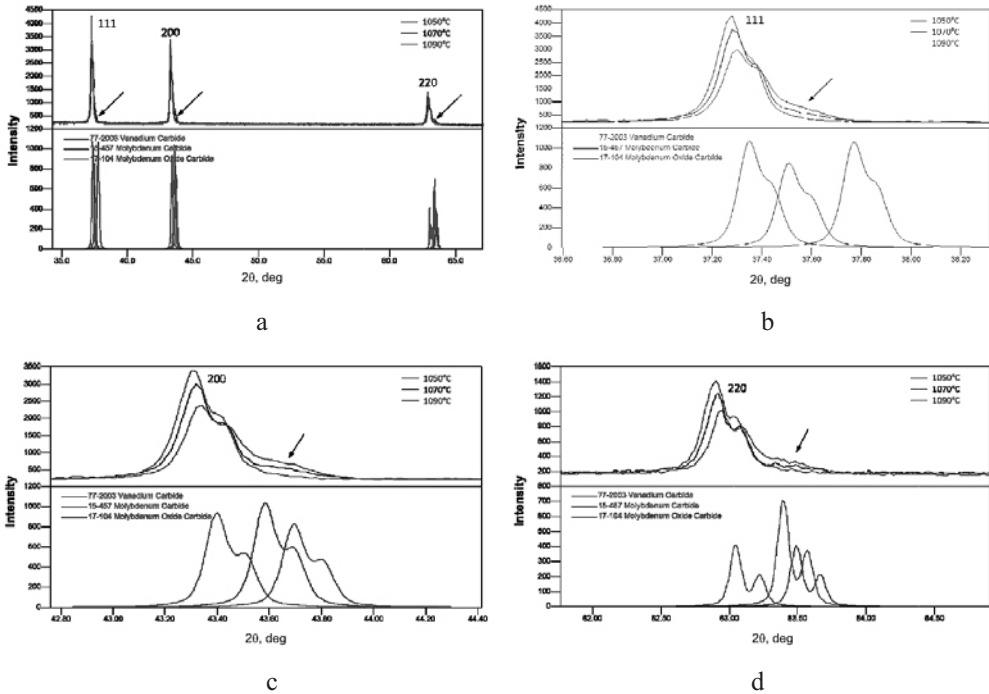

Fig. 4. XRD analysis of carbides of air quenched Hotvar steel showing the possible presence of molybdenum carbide (its peak is marked by arrows).

The cross-cuts of quenched specimens showed high hardness: 63–66 HRC irrespective of the austenizing temperature. Large hardness values are also related with the presence of dispersive carbides.

2.2. *Investigation of Bending Stress Effect on Martensitic Transformation.* At the moment of starting bending of air quenching specimen, the one is able to resist bending force as its yield strength is rather greater than bending stress that was just 100 MPa. The manufacture deals with the data concerning mechanical properties of Hotvar steel at high temperatures; however these are just tentative data as represent strength in quenched tempered steel (Table 3). The temperature during loading of specimen was measured to be 600°C (Fig. 5). The yield strength of quenched and tempered steels at 600°C is declared to be 830 MPa.

The manufacturer indicates [12] that martensitic transformation start temperature of Hotvar hot-work tool steel is about 220°C. The theoretical martensite start temperature was calculated according Capdevila et al. model [18] and it was obtained 267.42°C:

$$M_s(K) = 764.2 - 302.6w_C - 30.6w_{Mn} - 16.6w_{Ni} - 8.9w_{Cr} + 2.4w_{Mo} - 11.3w_{Cu} -$$

$$- 8.58w_{Co} - 7.4w_W - 14.5w_{Si}. \tag{1}$$

T a b l e 3

Mechanical Properties of Hotvar Steel at Elevated Temperatures [12]

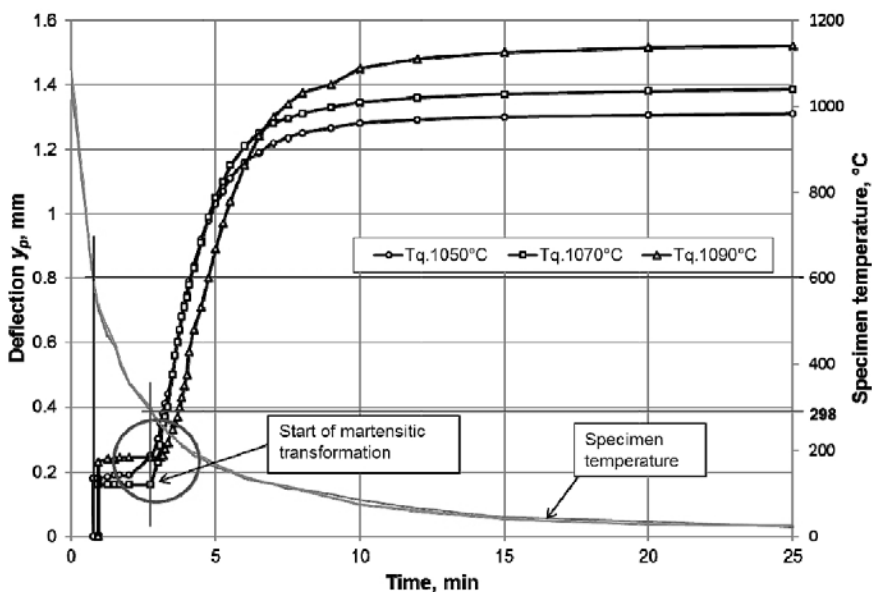| Test temperature (℃)	R_m, MPa	$R_{p0.2}$, MPa	Test temperature (℃)	R_m, MPa	$R_{p0.2}$, MPa
50	2300	1860	450	1760	1430
100	2200	1810	500	1650	1300
150	2130	1790	550	1450	1110
200	2060	1750	600	1180	830
250	2010	1710	650	800	520
300	1970	1690	700	350	210
350	1910	1600	750	200	100
400	1850	1510			

Fig. 5. Plastic deformation of specimens' air quenched from different austenizing temperatures.

Figure 5 shows that in our test the martensite transformation started when temperature of specimen dropped to 298℃, which is higher than that declared by manufacturer, as well as the calculated one. The reason of higher M_s can be the effect of stresses as it was found that tension and compression stimulate martensite transformation [19].

The intense bending of specimens began when temperature of the specimen had reached M_s (Fig. 5). At stress level $\sigma = 100$ MPa, the specimens' deflection amounted to 1.30, 1.39, and 1.52 mm, respectively, to austenizing temperature, during loading through air quenching. The higher temperatures were applied to specimens the greater deformations were obtained: when austenizing temperatures were 1070 and 1090℃, the plastic deflections exceeded the one obtained after quenching from 1050℃ by 8 and 15%, respectively (Fig. 5).

Deformation magnitude depends directly on the temperature of austenizing because at higher temperatures austenite has more dissolved carbides, and solid solution gets more

saturated with carbon and alloying elements. The principle role plays carbon dissolved in the austenite lattice.

Martensitic transformation is a non-diffusional process, so when it proceeds, all carbon dissolved in face-centred cubic (fcc) austenite lattice remains in the new phase – martensitic lattice saturated with carbon. It is known, that at room temperature α-iron may contain just up to 0.006% carbon, as austenite may reach even 2.14% [20]. During $\gamma \rightarrow \alpha$, the fcc lattice of austenite transforms to body-centred cubic (bcc) martensite lattice. Carbon atoms may occupy the sites of austenite lattice parallel to [100], [010], and [001] crystallographic directions. The transformation $\gamma \rightarrow \alpha$ is non-diffusional, therefore, during changes of fcc austenite lattice to bcc martensite lattice, carbon atoms remain inserted in martensite lattice only in [001] direction (and at the centers of planes parallel to (001)) thereby stretching the parameter c of tetragonal lattice [20].

So with increasing temperature of austenizing, more and more carbides are dissolved in austenite. As austenite becomes more rich in carbon atoms, the more of them intervene in [001] crystallographic directions. The carbon atoms create substantial strains or displacements of the neighboring iron atoms [21] and, therefore the specimens reach higher plastic deflections during bending. In this case, the stress effect on transformation plasticity of steel is just an instrumental way to show the transformation plasticity phenomenon as its conditioning was always a constant value.

The described theory requires the additional experiments as there is no undivided opinion about the relationship between parameters ratio c/a of tetragonal martensite lattice and carbon content in austenite and following martensite. Some researchers present the results of studies when the ratio c/a becomes larger than one only when the carbon content in austenite exceeds 0.6% [22, 23]. The Hotvar steel contains total amount of carbon of just 0.55%, moreover, the part of carbon is combined in carbides, so the carbon content remained in austenite is rather lower than the mentioned 0.6% limit. Hence, no matter how high austenizing temperature is, we could not reach the required carbon content for $c/a > 1$. As a result, the distance between adjacent iron atoms in martensite lattice in [001] crystallographic direction should not increase with rising austenizing temperature, so the same binds between atoms should occur. Hence, the plasticity should not increase, as well.

One can find other scientific works, where the opposite results were obtained. For example, Kremnev [24] indicated that quenching from various temperatures of high speed steel that contains 0.30, 0.42, and 0.43% of carbon in martensite, the ratio c/a of martensite lattice parameters was obtained greater than one, namely, 1.014–1.019 [24]. In this case, the interpretation of the increasing of steel plastic deflection dependent on austenizing temperature would be appropriate. Of course, influence of alloying elements on transformation plasticity needs to be checked, as it was also mentioned in [24].

For the purpose of developing the ideas of the carbon content influence on c/a ratio, the X-ray analysis was performed separately for the stretched and compressed surfaces of the specimen, also, a and c parameters were determined. The results are presented in Table 4. X-ray analysis showed that, in all cases, the ratio c/a was greater than 1. Furthermore, the differences of lattice parameters in stretched and compressed surfaces were revealed (see the last column of Table 4).

The main purpose of this research was to reveal the differences in phase transformations that occur during air quenching under tension and compression. We had a possibility to discover an effect of tension and compression on martensitic transformation. X-ray showed that intensities of martensite of compressed surfaces were of greater magnitude comparing to the ones of stretched layers (Fig. 6). This allows assumption that compression stimulates the martensitic transformation more than tension; moreover, this is in a good agreement with the results obtained by Fischlschweiger et al. [19].

Different influence of compression and tension was also determined by calculating the quantity of retained austenite in stretched and compressed layers by the XRD patterns of

T a b l e 4

Determination of Lattice Parameters for Stretched and Compressed Surfaces of Martensite after Air Quenching from Different Austenizing Temperatures

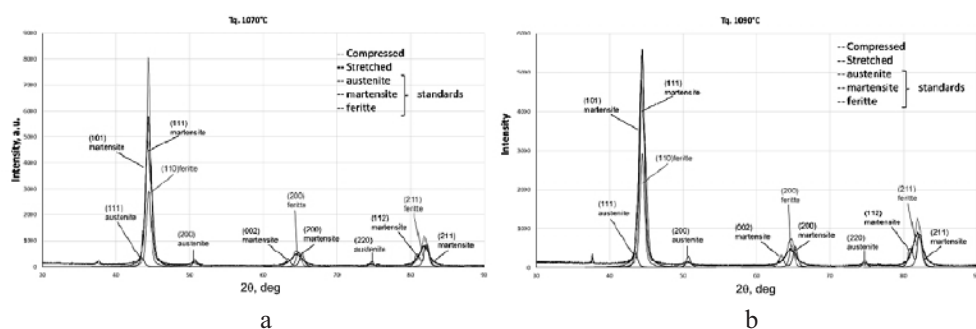| Austenizing temperature (°C)	Specimen surface	a, Å	c, Å	c/a	Difference between stretched and compressed
1050	Stretched	2.8504	2.8784	1.0098	
	Compressed	2.8506	2.8829	1.0113	More by 0.15%
1070	Stretched	2.8495	2.8808	1.0110	More by 0.08%
	Compressed	2.8509	2.8800	1.0102	
1090	Stretched	2.8537	2.8839	1.0106	More by 0.25%
	Compressed	2.8577	2.8809	1.0081	

Fig. 6. X-ray diffraction from stretched and compressed surfaces of specimen austenized at 1070 (a) and 1090°C (b).

steel. The calculation was made according to the ASTM E975 standard [25], where the following equation was used:

$$V_\gamma = (I_\gamma/R_\gamma)/[(I_\alpha/R_\alpha) + (I_\gamma/R_\gamma)], \qquad (2)$$

where V_γ and V_α are the volume fraction of γ- and α-phase, respectively (here α-phase means the volume of ferrite and martensite as the martensite peaks cannot be resolved from the ferrite peaks [26]), I_γ and I_α are the integrated intensity per angular diffraction peak (*hkl*) in the γ- and α-phase, respectively (they were calculated by taking the production of the maximum peak height and the peak width at half maximum height [27]), R_γ and R_α are the parameters depending on interplanar spacing (*hkl*), the Bragg angle, lattice parameters of the phases, R is defined as $(1/v_i^2)(FF^*)(LPF)pe^{-2M}$; the details of the calculation of R are described in [25–30].

According to the ASTM E975 [25], several methods of the calculation can be used such as choosing two peaks ($\alpha200$, $\gamma200$), three peaks ($\alpha200$, $\gamma200$, $\gamma220$) and four peaks ($\alpha200$, $\alpha211$, $\gamma200$, $\gamma220$). The peaks (110) of martensite and the (111) of austenite cannot be chosen because of overlapping [28]. The peaks ($\alpha200$, $\gamma200$) were chosen for calculation of retained austenite of steel.

All parameters required for calculation of volume of retained austenite is listed in Tables 5–7. The quantity of retained austenite in stretched and compressed layers is presented in Table 8. The calculation showed less quantity of austenite in compressed layers at all austenizing temperatures and confirms that compression stimulates martensitic

T a b l e 5

Determined Lattice Parameters used for Calculation of *R* Values

Austenizing temperature (℃)	Specimen surface	2θ, deg		Lattice parameter (Å)		
		Austenite	Martensite	Austenite	Martensite	
				a	*a*	*c*
1050	Stretched	50.48	64.36	3.598	2.8506	2.8829
	Compressed	50.66	64.66	3.601	2.8504	2.8784
1070	Stretched	50.82	64.50	3.590	2.8495	2.8808
	Compressed	50.42	64.46	3.617	2.8509	2.8800
1090	Stretched	50.54	64.68	3.596	2.8537	2.8839
	Compressed	50.72	64.56	3.597	2.8577	2.8809

T a b l e 6

Parameters of (200) Peaks of Austenite

Austenizing temperature (℃)	Specimen surface	2θ, deg	θ, deg	f	FF *	p	LPF	e^{-2M}	R_γ	I_γ
1050	Stretched	50.48	25.24	17.47	4885.08	6	8.56	0.94	107.90	100.09
	Compressed	50.66	25.33	17.48	5637.10	6	8.47	0.95	124.14	89.60
1070	Stretched	50.82	25.41	17.45	4873.47	6	8.41	0.94	108.50	136.32
	Compressed	50.42	25.21	17.52	4912.27	6	8.57	0.95	106.54	87.50
1090	Stretched	50.54	25.27	17.47	4881.21	6	8.44	0.94	107.99	94.50
	Compressed	50.72	25.36	17.52	4883.10	6	8.45	0.94	107.96	48.40

T a b l e 7

Parameters of (200) Peaks of Martensite

Austenizing temperature (℃)	Specimen surface	2θ, deg	θ, deg	f	FF *	p	LPF	e^{-2M}	R_γ	I_γ
1050	Stretched	64.36	32.18	15.27	932.56	6	4.92	0.92	45.03	744.85
	Compressed	64.66	32.33	15.23	927.96	6	4.88	0.92	43.90	660.33
1070	Stretched	64.50	32.25	15.29	934.77	6	4.92	0.92	46.10	715.20
	Compressed	64.46	32.23	15.28	933.27	6	4.93	0.92	46.10	771.50
1090	Stretched	64.68	32.34	15.23	927.61	6	4.88	0.91	45.00	436.30
	Compressed	64.56	32.28	15.16	919.30	6	4.90	0.92	44.90	738.90

transformation more than tension. The manufacture declares that after air quenching from 1050–1090℃ temperature, the quantity of retained austenite in Hotvar steel is 5% [12].

T a b l e 8

Calculated Quantity of Retained Austenite

Austenizing temperature (℃)	Quantity of austenite in layer of specimen (%)	
	Stretched	Compressed
1050	5.3	4.9
1070	6.5	4.7
1090	5.6	2.7

At the air quenching of specimens after heating at austenizing temperature martensitic transformation did not begin immediately, but after 3–4 minutes when the specimen was withdrawn from the furnace, i.e., when the temperature dropped to 220–250℃. This was clearly seen when the specimens started to bend immediately after heating (Fig. 5). When the specimen started bending already during the originated martensite transformation, i.e., at 4th or 5th minute of cooling, they immediately began bending (Fig. 7). However, the deflections were nearly 30–40% lower than in the first case (see the total deflection at Fig. 5). Later loading of specimens resulted in a higher loss of plasticity, because at the last stage of the transformation, the nuclear binds became stronger.
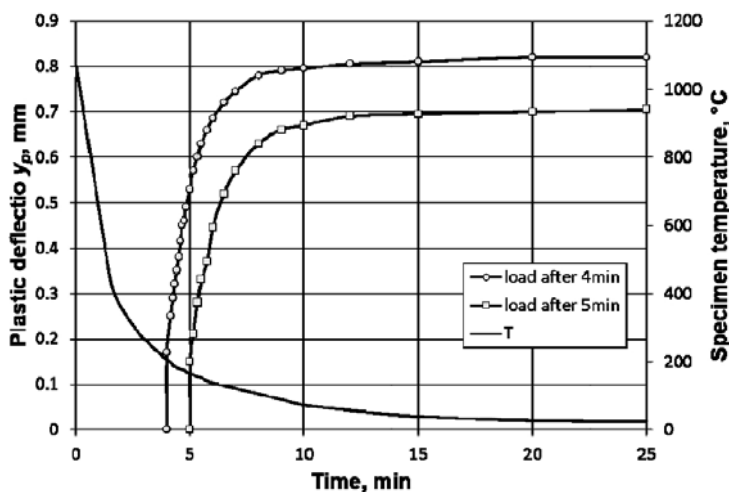

Fig. 7. Plastic deformation of specimens after bending that began at 4th and 5th minutes of cooling. Austenizing temperature 1070℃.

2.3. *Self-Deformation of Steel*. An interesting phenomenon has been observed, when steel specimens were unloaded at the beginning of the air quenching, i.e., at 4th or 5th minutes of the test, and the monitoring of deflection of specimen was continued. It was noted that curved and unloaded specimens successfully bent in the same direction as they were bent, but with a less intensity (Fig. 8). In this case, the external stress has a direct impact on transformation plasticity passing as bending load generated compression and tension stresses in specimen at the same moment. Compression stimulates martensitic transformation more than tension as compressed surfaces of specimens' show higher diffraction intensities for martensite.

The influence of tension and compression stresses that were generated in the specimens is different for the martensitic transformation start temperature M_s and its intensity. This phenomenon is related to anisotropy of volume changes that creates
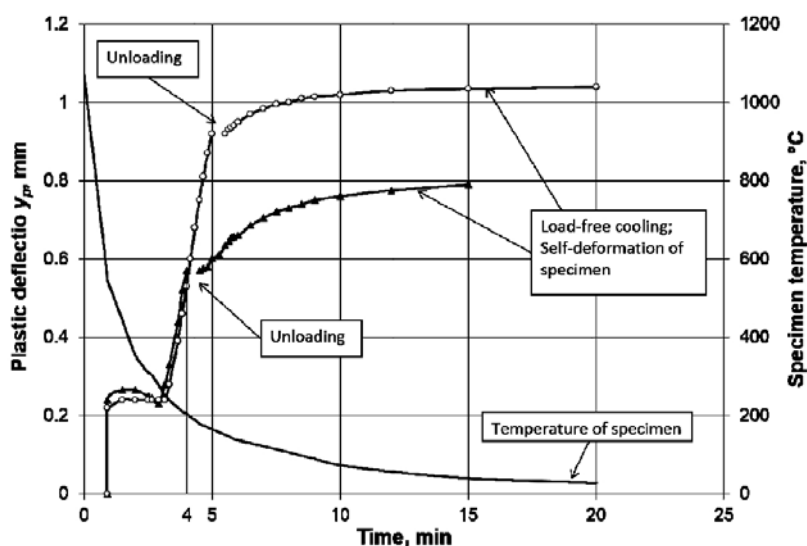
Fig. 8. The phenomenon of self-deformation of Hotvar steel after unloading of specimens bent and air quenched from 1070°C.

self-deformation of steel parts, so called, self-deformation, even in that way, when the value of external stresses is $\sigma = 0$ [11].

The self-deformation of bent, unloaded at the certain moment and exposed to the following load-free cooling specimens has reached about 28 and 12% of plastic deflection when specimen was unloaded at 4 or 5 min of total cooling time, respectively.

Altogether, martensitic transformation is very sensitive to stress, thus, deforming the initial structure – austenite, the martensitic transformation occurs at higher temperatures than M_s [6]. In addition, it was found that at the quenching of steel, the transformations (decomposition of austenite and self-tempering of martensite) proceeds at different stages in stretched and compressed sides [31]. Therefore, it must be assumed that the tensile and compressive stresses exhibit different effects on quenching and tempering transformations. As the bent and unloaded specimens get curved further at the cooling process, the stretched volume of specimens is increased. It was determined that the specific volume of austenite is the smallest, and the one of martensite is the largest [6, 20].

Obviously, that martensitic transformation was inhibited in stretched volume of specimen, so, unloading was following by increasing of volume as the result of intensive formation of new martensite crystals. Decomposition of austenite into martensite inside the compressed part of specimen has started before, so its proceeding has been interrupted. When transformation performs at different intensities, the volumetric changes can make the specimen to bend to one or other one. The value of deflection alteration has shown the quantitative differences in transformations.

C o n c l u s i o n s

1. Microstructure of Hotvar tool steel air quenched from 1050–1090°C temperature is composed of martensite, carbides, mainly of vanadium and molybdenum, and small content of retained austenite (3–6%).

2. The transformation plasticity of Hotvar tool steel specimens increases from 8 to 15% when austenizing temperature rises from 1050 to 1090°C, respectively. It is quite possible that interstitial carbon atoms positioned in [001] crystallographic direction have the main influence on reducing the atomic binds.

3. The air quenched Hotvar steel has slightly tetragonal lattice. The influence of tension and compression on the c/a ratio is different – usually, the stretched surfaces showed higher magnitudes of c/a.

4. The transformations that occur during air quenching are dependent on stress mode. X-ray analysis revealed that the compressed layers had higher contents of martensite. The content of retained austenite was determined 2.7–4.9 and 5.3–6.5% in compressed and stretched layers of specimens depending on austenizing temperature.

5. It was determined that the loss of transformation plasticity is about 30–40% when the bending was started at temperatures lower than M_s.

6. The specimens were self-bending in the same direction as they were bent when the load was removed at the temperatures below M_s. It proves assumption that the stretched side of specimen had less martensite comparing to the compressed one at the moment of unloading.

Р е з ю м е

Досліджується зміна пластичності та мікроструктури жароміцної інструментальної сталі при мартенситному перетворенні. Зразки піддавали астенітизації та закалюванню на повітрі. У процесі охолодження їх навантажували статичним згином із номінальним напруженням 100 МПа за трьома схемами: статичний згин зразків після їх вилучення з печі, при цьому відмічались деформація початкового аустеніту і формування мартенситу під дією навантаження; згин після початку мартенситного перетворення з деформацією мартенситу; розвантаження з моменту початку мартенситного перетворення з переважаючою деформацією аустеніту, при цьому вимірювалась деформація при розвантаженні. При охолодженні зразків до кімнатної температури вимірювалась величина їх пластичного прогину. Показано, що мартенситне перетворення характеризується суттєвим підвищенням пластичності. Різний вплив на мартенситне перетворення розтяжних і стискальних напружень оцінювали шляхом вимірювання деформації зразків при розвантаженні. Мікроструктура розтягнутих і стиснутих поверхонь зразків досліджувалась методами рентгенівської дифрактометрії, електронної мікроскопії і електронно-дисперсійної спектроскопії.

1. Z. Gronostajski, M. Kaszuba, M. Hawryluk, and M. Zwierzchowski, "A review of the degradation mechanisms of the hot forging tools," *Arch. Civil Mech. Eng.*, **14**, 528–539 (2014).

2. A. Medvedeva, J. Bergström, S. Gunnarsson, and J. Anderson, "High-temperature properties and microstructural stability of hot-work tool steels," *Mater. Sci. Eng. A*, **523**, 39–46 (2009).

3. E. Brinksmeier, Th. Lübben, U. Fritsching, et al., "Distortion minimization of disks for gear manufacture," *Int. J. Mach. Tools Manuf.*, **51**, 331–338 (2011).

4. J. R. Cho, W. J. Kang, M. G. Kim, et al., "Distortions induced by heat treatment of automotive bevel gears," *J. Mater. Process. Technol.*, **153-154**, 476–481 (2004).

5. K. Amini, A. Akhbarizadeh, and S. Javadpour, "Investigating the effect of the quench environment on the final microstructure and wear behaviour of 1.2080 tool steel after deep cryogenic heat treatment," *Mater. Design*, **45**, 316–322 (2013).

6. Yu. M. Lachtin and V. P. Leont'eva, *Materials Science. Handbook* [in Russian], Mashinostroenie, Moscow (1980).

7. R. K. Janutienė, "The investigation of plasticity and microstructure of Hotvar steel during martensitic transformation," in: Proc. of Europ. Conf. on Heat Treatment and 21st IFHTSE Congress (Munich, Germany, 2014), pp. 407–414.

8. N. Ausmanas, R. K. Janutienė, and J. Žvinys, "Investigation of plastic properties of Hotvar hot work tool steel during martensitic transformation," *Mater. Sci. (Medžiagotyra)*, **21**, No. 1, 18–22 (2015).

9. R. K. Janutienė and J. Žvinys, "Low carbon chromium steel transformation plasticity during tempering," *Mater. Sci. (Medžiagotyra)*, **12**, No. 2, 101–105 (2006).

10. J. Žvinys and R. K. Janutienė, "Carbon and tempering temperature influence on steel kinetic plasticity," *Mater. Sci. (Medžiagotyra)*, **6**, No. 3, 172–174 (2000).

11. A. I. Tyshchenko, W. Theisen, A. Oppenkowski, et al., "Low-temperature martensitic transformation and deep cryogenic treatment of a tool steel," *Mater. Sci. Eng. A*, **527**, 7027–7039 (2010).

12. *Uddeholm Hotvar*, http://www.uddeholm.com/files/hotvar-english.pdf.

13. H. Kim, J. Lee, F. Barlat, et al., "Experiment and modeling to investigate the effect of stress state, strain and temperature on martensitic phase transformation in TRIP-assisted steel," *Acta Mater.*, **97**, 435–444 (2015).

14. H. K. Yeddu, A. Borgenstam, and J. Ågren, "Stress-assisted martensitic transformations in steels: A 3-D phase-field study," *Acta Mater.*, **61**, 2595–2606 (2013).

15. W. Kraus and G. Nolze, "POWDER CELL – a program for the representation and manipulation of crystal structures and calculation of the resulting X-ray powder patterns," *J. Appl. Cryst.*, **29**, 301–303 (1996).

16. *DIFFRACplus. v15.0: EVA (2009) – User's Manual*, Bruker AXS, Karlsruhe, Germany (2009).

17. M. Maalekian, M. L. Lendinez, E. Kozeschnik, et al., "Effect of hot plastic deformation of austenite on the transformation characteristics of eutectoid carbon steel under fast heating and cooling conditions," *Mater. Sci. Eng. A*, **454-455**, 446–452 (2007).

18. C. Capdevila, F. G. Caballero, and C. Garcia Andres, "Determination of M_s temperature in steels: A Bayesian neural network model," *ISIJ Int.*, **42**, No. 8, 894–902 (2002).

19. M. Fischlschweiger, Th. Antretter and G. Cailletaud, "Transformation hardening and kinetics for stress assisted and temperature driven martensitic transformation in steels," *Mech. Res. Commun.*, **47**, 84–88 (2013).

20. I. I. Novikov, *Theory of Heat Treatment of Metals* [in Russian], Metallurgiya, Moscow (1978).

21. G. Krauss, "Martensite in steel: strength and structure," *Mater. Sci. Eng. A*, **273-275**, 40–57 (1999).

22. O. D. Sherby, J. Wadsworth, D. R. Lesuer, and Ch. K. Syn, "The c/a ratio in quenched Fe–C and Fe–N steels – a heuristic story," in: Proc. of Conf. THERMEC 2006 (July 4–8, 2006, Vancouver, Canada), https://e-reports-ext.llnl.gov/pdf/329979.pdf.

23. O. D. Sherby, J. Wadsworth, D. R. Lesuer, and Ch. K. Syn, "Revisiting the structure of martensite in iron-carbon steels," *Mater. Trans.*, **49**, No. 9, 2016–2027 (2008).

24. L. S. Kremnev, "Influence of steel alloying components on martensite tetragonality," http://arxiv.org/ftp/ arxiv/papers/1108/1108.3420.pdf.

25. *ASTM E975-13. Standard Practice for X-Ray Determination of Retained Austenite in Steel with Near Random Crystallographic Orientation*, ASTM International, West Conshohocken, PA (2013).

26. T. Gnäupel-Herold and A. Creuziger, "Diffraction study of the retained austenite content in TRIP steels," *Mater. Sci. Eng. A*, **528**, 3594–3600 (2011).

27. K. Norrish and R. M. Taylor, "Quantitative analysis by X-Ray diffraction," *Clay Miner.*, **5**, 98–109 (1962).

28. Y.-Y. Su, L.-H.Chiu, T.-L.Chuang, et al., "Retained austenite amount determination comparison in JIS SKD11 steel using quantitative metallography and X-Ray diffraction methods," *Adv. Mater. Res*., **482-484**, 1165–1168 (2012).

29. M.-X. Zhang, P. M. Kelly, L. K. Bekessy, and J. D. Gates, "Determination of retained austenite using an X-Ray texture goniometer," *Mater. Character.*, **45**, 39–49 (2000).

30. Ch. Kim, "X-Ray method of measuring retained austenite in heat treated white cast irons," *J. Heat Treat*., **1**, No. 2, 43–51 (1979).

31. R. K. Janutienė, J. Žvinys, and A. Baltušnikas, "Influence of bending stress on microstructure of tempered high chromium steel," *Mater. Sci.* (*Medžiagotyra*), **10**, No. 3, 201–205 (2004).